



PAPER • OPEN ACCESS

Theoretical and simulation analysis of piezoelectric liquid resistance captor filled with pipeline

To cite this article: Li Zheng *et al* 2018 *Mater. Res. Express* **5** 035517

View the [article online](#) for updates and enhancements.

You may also like

- [Design and investigation on a novel piezoelectric screw pump](#)
Yongkang Yin, Chunhua Zhou, Fagang Zhao et al.
- [An adjustable magnetic type resonant multimodal inertial impact motor](#)
Liangguo He, An Qian, Xinyu Li et al.
- [A novel multifunctional piezoelectric composite device for mechatronics systems by using one single PZT ring](#)
Guangqing Wang, Zexiang Zhao, Jiangping Tan et al.

Breath Biopsy Conference



5th & 6th November
Online

BREATH
BIOPSY



Join the conference to explore the **latest challenges** and advances in **breath research**, you could even **present your latest work!**

Register now for free!



Main talks

Early career sessions

Posters



PAPER

Theoretical and simulation analysis of piezoelectric liquid resistance captor filled with pipeline

OPEN ACCESS

RECEIVED

11 December 2017

REVISED

2 February 2018

ACCEPTED FOR PUBLICATION

15 March 2018

PUBLISHED

28 March 2018

Original content from this work may be used under the terms of the [Creative Commons Attribution 3.0 licence](#).

Any further distribution of this work must maintain attribution to the author(s) and the title of the work, journal citation and DOI.

Li Zheng^{1,2,6} , Yang Zhigang¹, Kan Junwu³, Lisheng⁴, Yan Bo² and Lu Dan⁵¹ College of Mechanical Science and Engineering, Jilin University² College of Civil Engineering, Jilin Jianzhu University³ College of Mathematics Physics and Information Engineering, Zhejiang Normal University⁴ Chemical Co Ltd, Liaoyang⁵ DeGuan Education School, JiLin⁶ Author to whom any correspondence should be addressedE-mail: leepangzi@163.com**Keywords:** electromechanical equivalent model, modeling, simulation, circular piezoelectric vibrator, power generation**Abstract**

This paper designs a kind of Piezoelectric liquid resistance capture energy device, by using the superposition theory of the sheet deformation, the calculation model of the displacement curve of the circular piezoelectric vibrator and the power generation capacity under the concentrated load is established. The results show that the radius ratio, thickness ratio and Young's modulus of the circular piezoelectric vibrator have greater influence on the power generation capacity. When the material of piezoelectric oscillator is determined, the best radius ratio and thickness ratio make the power generation capacity the largest. Excessive or small radius ratio and thickness ratio will reduce the generating capacity and even generate zero power. In addition, the electromechanical equivalent model is established. Equivalent analysis is made by changing the circuit impedance. The results are consistent with the theoretical simulation results, indicating that the established circuit model can truly reflect the characteristics of the theoretical model.

1. Introduction

With the increasing emphasis on industrial intelligence, small and portable wearable smart devices and portable products including MEMS, wireless sensor system, embedded system and wireless communication technology have been popularized and applied [1] rapidly. In these systems, the life of the system does not depend on the wear degree of the mechanical parts in the system, but on the service life of the power supply devices, especially in the electromechanical system that is difficult to replace the power supply. Furthermore, although tiny intelligent device only occupies less space, but the number of electronic components in these systems are numerous and complex distribution applications it will inevitably have to consume more energy, energy supply problems facing major challenges, the original offer for these components of intelligent energy supply is large in size, lower power density, limited service life, and can not be integrated in the micro system, it is difficult to meet the demand for the use of portable electronic devices, although the micro high performance battery in service life and energy density to improve the performance, but the supply of life is limited, so limiting the current application of [2–4] MEMS products, the rapid development of wireless sensor network and embedded system. How to convert the energy in the environment into electrical energy and power [5–7] for all kinds of low power electronic components all day long. How to further improve the ability of vibration isolation and vibration reduction for smart components has been attracting more and more attention. It has become a hot research topic and urgent problem at home and abroad at present [8–13].

Anderson improves the damping capacity of [7] by the method of adding transverse beam manufacturing in the deep shallow water sloshing damper, Marsh studied the effect of depth and width of the liquid container of shallow water sloshing damping damping effect, that the energy consumption of the traveling wave is much larger than the standing wave, so the sloshing damping effect is better than the traveling wave standing wave sloshing [8]. In 2006, Wu Baichang and Beihang University put forward a new type of piezoelectric ceramic solid liquid actuator [9], taking oil as the transmission medium, and analyzed its performance.

In 2012, Ori Ehrenberg and Gabor Kosa of the Department of mechanical engineering, Tel Aviv University, Israel proposed a micropump [10] driven by a traveling wave driven by a tubular piezoelectric actuator. In general, a liquid mixer consists of two separate parts of a fluid pump and a mixer, but the invention of a piezoelectric pump makes it possible to combine the two. In 2012, France's M Deterre [14] made a similar study, proposes a method for active implantable medical devices using piezoelectric self powered, low frequency pressure film recycling fluid environment can.

In March 2010, Jiang Delong and others at Jilin University designed the piezoelectric double chip parallel piezoelectric pump [15]. In 2010, Jilin University, Fan Zunqiang and so on put forward a new type of piezoelectric linear precision stepping motor [16].

From the structure of the pump, the Jung-HoPark and others of Tokyo Institutet of Technology have developed and reported a kind of large flow micro pump [17, 18]. Driven by the square wave of 100 V and 2 kHz, the micro pump can obtain the maximum flow rate 80 ml s^{-1} , the maximum output pressure 0.32 MPa and the maximum output power 0.8 mW.

SONU Rujun, SHAN Xiaobiao [19, 20]. The influence of the coupling between the fluid environment and the pow is studied. Vibration is everywhere in the daily environment. The frequency of vibration is mostly from several hertz to dozens of Hertz [21], and the natural frequency of the piezoelectric chip is thousands of Hertz. How to improve the energy recovery and utilization of the piezoelectric wafer in the environment has become the current research hotspot [22–24]. Xu Hui [25–27], the damping mechanism of bionics, fluid and solid dynamics theory of passive control based on a new design, put forward a kind of passive control theory a new embedded self moving mass adaptive damping theory, and its application in vibration control of beam and slab, achieved good damping effect. Based on experiments, we have studied the adaptive damping system of the Euler beam embedded with viscous fluid under the excitation of main resonance, and analyzed the characteristics of fluid motion and wall pressure curve in depth. In view of the simplified dynamic boundary fluid dynamic model, a quantitative index is proposed to determine the effect of damping from the angle of the energy consumption of the fluid motion.

Kan Junwu [28] *et al.* Proposed a new type of pressure fluid coupling vibration of piezoelectric hydraulic transducer based on the transducer with the joint power hydraulic fluid medium to transfer movement and power to realize the multi vibrator structure, high power, low frequency power device for piezoelectric energy can provide a basis for further research of hydraulic control technology vibration.

According to the research status of piezoelectric transducer and power supply since the new demand of vibration control, the author puts forward the gas/liquid coupling effect of piezoelectric vibration energy harvester based on [29], the advantages of fluid buffer, which can avoid the piezoelectric vibrator by rigid impact and high reliability; easy to flow through the lower back pressure adjusting the system stiffness and frequency, can realize low-frequency, broadband vibration energy recovery; easy to realize multi piezoelectric oscillator synchronization, power generation capacity. In addition, the type of power capture has the effect of vibration suppression at the same time.

Research and development of dynamic through understanding of fluid filled pipe vibration and piezoelectric drive obtained in the field, in summarizing and absorbing the basis of previous experience, the fluid filled pipe system and vibration control for piezoelectric vibration characteristics analysis put forward a new type of piezoelectric hydraulic damper, it uses resonance current piezoelectric materials for the attenuation of fluid pulsation, the piezoelectric and fluid coupling to realize vibration energy recovery, vibration absorption and energy recovery characteristics and combined with theoretical analysis and numerical simulation to study the shock absorber.

2. Structure and working principle of hydraulic power trapping device for liquid filled pipe

This paper describes the design of a liquid filled pipe piezoelectric liquid resistance transducer structure as shown in figure 1, which uses the circular mass and piston rod as the amplification mechanism, the source of driving the hydraulic cylinder to simulate fluid flow under vibration, the vibration of liquid through the amplification mechanism to the piezoelectric film, because the fluid, the spring and the piezoelectric transducer has a liquid resistance vibration absorbing and buffering effect, resulting in the hydraulic cylinder piston (by vibration object) vibration and piezoelectric vibration is not consistent, so that the liquid is controlled by vibration isolation because of inconsistent objects; vibration caused by pipe cavity volume changes frequently. Will this change the liquid passes through the pipeline to the piezoelectric transducer in the piezoelectric vibrator produces alternating deformation, the deformation of the piezoelectric vibrator alternately converts mechanical energy into electrical energy, part of the vibration energy recovery system. Liquid filled pipe piezoelectric haversters liquid resistance system using liquid medium to absorb vibration transmission, and the use of piezoelectric vibrator capture energy, can make the vibration isolation of the object to be controlled, and can reclaim vibration energy, can achieve more efficiency. Composed of the piezoelectric vibrator of the simple

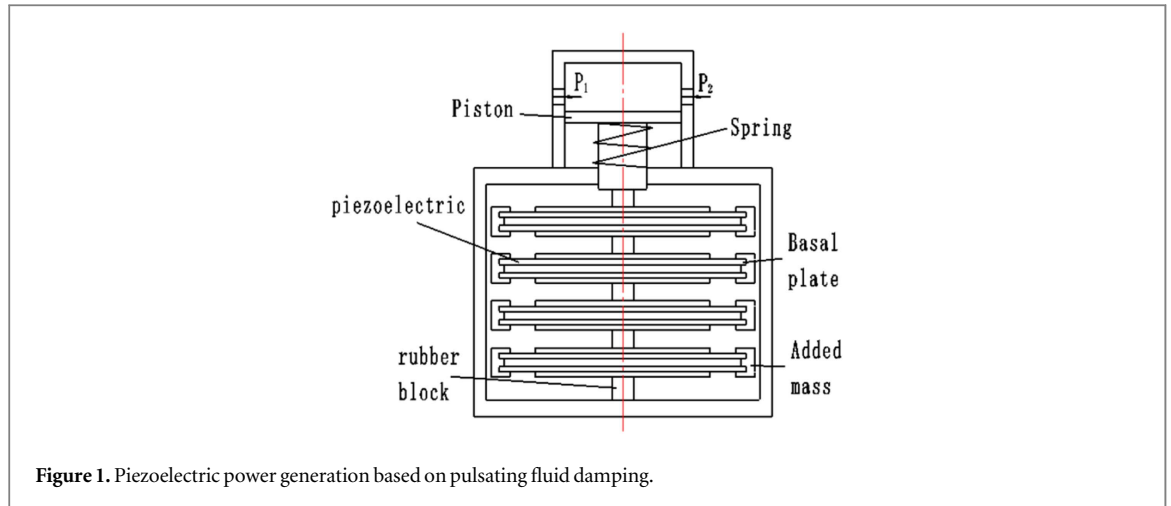


Figure 1. Piezoelectric power generation based on pulsating fluid damping.

vibration harvesting traditional energy is different, to achieve the transfer of movement and energy coupling of piezoelectric body and the fluid in this paper, to achieve a variety of piezoelectric vibrator working together, especially can be used for energy recovery, low frequency and large amplitude vibration environment. Under the boundary condition of uniformly distributed external load, the circular piezoelectric vibrator is deformed under the action of elastic support and concentrated load in the center. The center and outer edge of the same surface are different from stress (tensile stress and compressive stress).

When the piezoelectric wafer diameter is larger, and the piezoelectric vibrator with a surface and generate positive and negative charge generating capacity will be greatly reduced, or even no power output (positive and negative offset); on the other hand, the center part of the piezoelectric wafer generated electrical energy increases with the increase of its radius. Therefore, when the outer edge of the piezoelectric substrate at the pressure node electric vibrator deformation, the maximum power output (the surface of the piezoelectric wafer only by a stress), and the radius of nodes (i.e. the optimal radius of the piezoelectric wafer) depends on many elements of the piezoelectric vibrator, thickness, material the boundary conditions and incentives.

According to the plate and shell theory, the bending deformation curve and deformation volume of the simply supported boundary piezoelectric vibrator (figure 2) under uniformly distributed fluid pressure are respectively.

An intermediate point supporting circular plate is desirable: for an integral circular plate with a simply supported outer boundary ($r = b$) and an outer boundary ($r = a$) as a simple boundary, the vibration modes can be expressed in two parts:

The inner circle of $0 \leq r \leq b$, under a concentrated load in the middle, around the whole plate for free. In the outer ring of $b \leq r \leq a$, according to the circular plate is circle free inner circle simply supported. The distance between the bottom and the neutral layer of the metal substrate can be obtained from the reference [30]:

$$h_z = \frac{E_m h_m^2 / (1 - \nu_m^2) + E_p (h^2 - h_m^2) / (1 - \nu_p^2)}{2[E_m h_m / (1 - \nu_m^2) + E_p h_p / (1 - \nu_p^2)]} = \alpha h \quad (1)$$

Form $\alpha = \frac{\zeta(1 - \beta)^2(1 - \nu_p^2) + [1 - (1 - \beta)^2](1 - \nu_m^2)}{2[\zeta(1 - \beta)(1 - \nu_p^2) + \beta(1 - \nu_m^2)]}$, E_m , E_p are the modulus of elasticity of metal substrates and piezoelectric ceramics, $\zeta = E_m / E_p$ is defined as the young's modulus ratio of piezoelectric vibrators; ν_p and ν_m are the Poisson ratio of piezoelectric ceramic materials and metal substrates.

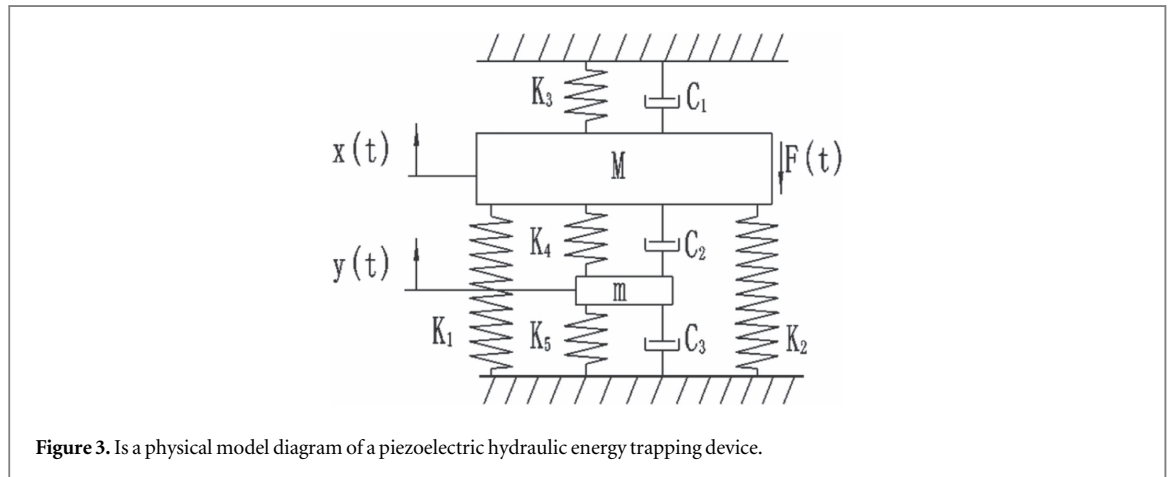
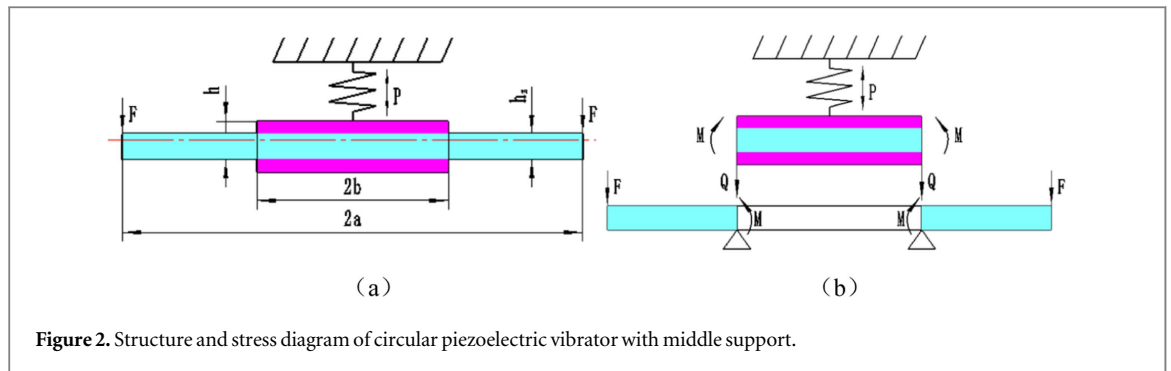
Referring to material science and piezoelectricity knowledge, the internal stress and electric field strength of piezoelectric ceramics can be expressed respectively as an external force:

$$T_1 = \frac{E_p}{1 - \nu_p^2} (S_1 + \nu_p S_2) - \frac{g_{31} E_p}{1 - \nu_p} D_3 \quad (2)$$

$$T_2 = \frac{E_p}{1 - \nu_p^2} (S_2 + \nu_p S_1) - \frac{g_{31} E_p}{1 - \nu_p} D_3 \quad (3)$$

$$S_1 = z \frac{d^2 w}{dr^2} \quad (4)$$

$$S_1 = z \frac{d^2 w}{dr^2} \quad (5)$$



$$E_3 = -g_{31}(T_1 + T_2) + \beta_{33}^T D_3 \tag{6}$$

Form S_1 and S_2 respectively, radial strain and tangential strain; T_1 and T_2 respectively, the radial stress and tangential stress; G_{31} piezoelectric constant (voltage); R is the radius of curvature; potential D_3 for Z direction shift; E_3 electric field strength is Z direction; for the dielectric isolation rate.

Figure 3 is a physical model diagram of a piezoelectric liquid energy harvesting device, the sum of the additional mass and liquid mass at the drive end of the pipeline system, expressed in M , The additional mass around the piezoelectric oscillator and oscillator is represented by m , K_1 is the stiffness of the loaded spring, K_2 and c_1 are the equivalent stiffness and damping of the liquid, $k_3 = k_4 = k_p \cdot n/2$ is the equivalent stiffness of series piezoelectric vibrators, $c_2 = c_3$ is the equivalent damping of series piezoelectric vibrators, n is the number of drum type piezoelectric vibrators, and the external excitation is expressed by $F(t)$ ignoring the influence of the pipeline on the system.

As shown, the absolute displacement of mass blocks is expressed by $x_1(t)$ and $x_2(t)$ which represents the absolute displacement of the surrounding mass in the piezoelectric fluid blocking energy device. The $F(t)$ is the excited force, and the following equations of motion can be obtained:

$$m_1 \ddot{x}_1 - (c_1 + c_2) \dot{x}_1 + c_2 \dot{x}_2 - (k_1 + k_2 + k_3)x_1 + k_3 x_2 = F(t) \tag{7}$$

$$m_2 \ddot{x}_2 + c_2 \dot{x}_1 - (c_2 + c_3) \dot{x}_2 + k_3 x_1 - (k_3 + k_4)x_2 = 0 \tag{8}$$

The piezoelectric energy harvesting device in the hydraulic resistance of piezoelectric vibrator structure is the same, the quality of M is M_1 , the quality of block m is m_2 , the vibration source ω is the angular frequency of displacement, this chapter selects the external incentives in the form of sinusoidal harmonic excitation, i.e., M steady state response can be obtained:

$$X_1 = H \sqrt{\frac{(1 + \omega_{22})^2 + \xi_{12}^2}{a^2 + b^2}} \tag{9}$$

$$X_2 = \sqrt{\frac{(\xi_{21} + \omega_{21} + \xi_{21}\omega_{22} + \omega_{21}\omega_{22})^2 + \xi_{22}^2(\xi_{21} + \omega_{21})^2}{(1 + \omega_{22})^2 + \xi_{22}^2}} H \sqrt{\frac{(1 + \omega_{22})^2 + \xi_{12}^2}{a^2 + b^2}} \tag{10}$$

$$\begin{aligned} \text{其中, } H &= -\frac{F}{m_1\omega^2}, a = 1 + \omega_{22} + \xi_{11}\xi_{22} + \omega_{11} + \omega_{22}^2 - \omega_{12}\xi_{21} - \omega_{12}\omega_{21}, \\ b &= \xi_{22} - \xi_{11} - \xi_{11}\omega_{22} - \xi_{12}\xi_{21} - \xi_{12}\omega_{21} + \xi_{22}\omega_{11}, \xi_{11} = \frac{c_1 + c_2}{m_1\omega}, \xi_{12} = \frac{c_2}{m_1\omega}, \omega_{11} = \frac{k_1 + k_2 + k_3}{m_1\omega^2}, \\ \omega_{12} &= \frac{k_3}{m_1\omega^2}, \xi_{21} = \frac{c_2}{m_2\omega}, \xi_{22} = \frac{c_2 + c_3}{m_2\omega}, \omega_{21} = \frac{-k_3}{m_2\omega^2}, \omega_{22} = \frac{k_3 + k_4}{m_2\omega^2}. \end{aligned}$$

Each piezoelectric vibrator has the same structure, and the mass displacement is uniformly distributed among the piezoelectric vibrators, and their central deformation is as follows:

$$\delta = X_2/2n = \sqrt{\frac{(\xi_{21} + \omega_{21} + \xi_{21}\omega_{22} + \omega_{21}\omega_{22})^2 + \xi_{22}^2(\xi_{21} + \omega_{21})^2}{(1 + \omega_{22})^2 + \xi_{22}^2}} H \sqrt{\frac{(1 + \omega_{22})^2 + \xi_{12}^2}{a^2 + b^2}} / 2n \quad (11)$$

According to the relationship between the charge and the voltage, the open circuit voltage generated by the piezoelectric vibrator under the action of external force is as follows:

$$V_g = \frac{Q_g}{C_f} = \frac{(1 - \gamma) \cdot (2 - 2\alpha - \beta) \cdot \beta \cdot g_{31} \cdot E_p \cdot h^2 \cdot P}{4 \cdot \pi \cdot (1 - \nu_p) \cdot (1 + \nu_c) \cdot D_c} \quad (12)$$

The equivalent stiffness of each piezoelectric vibrator is k_p , and the central point deformation is δ , and then there is $P = k_p \cdot \delta$, which is substituted into the formula (13).

$$\begin{aligned} V_g &= \frac{Q_g}{C_f} = \frac{(1 - \gamma) \cdot (2 - 2\alpha - \beta) \cdot \beta \cdot g_{31} \cdot E_p \cdot h^2 \cdot k_p \cdot \delta}{4 \cdot \pi \cdot (1 - \nu_p) \cdot (1 + \nu_c) \cdot D_c} \\ &= \frac{(1 - \gamma) \cdot (2 - 2\alpha - \beta) \cdot \beta \cdot g_{31} \cdot E_p \cdot h^2 \cdot k_p \cdot X_2}{4 \cdot \pi \cdot (1 - \nu_p) \cdot (1 + \nu_c) \cdot D_c \cdot n} \end{aligned} \quad (13)$$

The power generated by a single piezoelectric vibrator is:

$$\begin{aligned} U_g &= \frac{1}{2} C_f V_g^2 = \frac{\beta h^3}{32\pi\beta_{33}^S} \left[\frac{g_{31} \cdot E_p (1 - \gamma) \cdot (2 - 2\alpha - \beta) \cdot \lambda \cdot a \cdot P}{(1 - \nu_p) \cdot (1 + \nu_c) \cdot D_c} \right]^2 \\ &= \frac{\beta h^3}{32\pi\beta_{33}^S} \left[\frac{g_{31} \cdot E_p (1 - \gamma) \cdot (2 - 2\alpha - \beta) \cdot \lambda \cdot a \cdot k_p \cdot X_2}{2 \cdot n \cdot (1 - \nu_p) \cdot (1 + \nu_c) \cdot D_c} \right]^2 \end{aligned} \quad (14)$$

The total power generation of the piezoelectric hydraulic energy harvesting device is as follows:

$$\begin{aligned} U_S &= 2nU_g = nC_f V_g^2 = 2n \cdot \frac{\beta h^3}{32\pi\beta_{33}^S} \left[\frac{g_{31} \cdot E_p (1 - \gamma) \cdot (2 - 2\alpha - \beta) \cdot \lambda \cdot a \cdot P}{(1 - \nu_p) \cdot (1 + \nu_c) \cdot D_c} \right]^2 \\ &= \frac{\beta h^3}{64\pi\beta_{33}^S} \left[\frac{g_{31} \cdot E_p (1 - \gamma) \cdot (2 - 2\alpha - \beta) \cdot \lambda \cdot a \cdot k_p \cdot X_2}{(1 - \nu_p) \cdot (1 + \nu_c) \cdot D_c} \right]^2 \end{aligned} \quad (15)$$

The formula (15) shows that the power performance of the electro-hydraulic pressure resistance device not only by the circular piezoelectric vibrator structure, influence of piezoelectric material parameters, but also by the mass, the drum type piezoelectric vibrator of the external excitation frequency and the number of groups.

3. Simulation analysis of the power generation performance of a liquid filled pipe piezo trap

In this paper, the fluid pipes of piezoelectric power generation characteristics of liquid resistance transducer of power generation performance for external vibration to the transducer to achieve optimal, the power performance of the frequency response analysis, find the law of influence of various factors on the transducer voltage power frequency response curve, then the external vibration has know, by adjusting the parameters of the power to achieve optimal performance. This section focuses on the analysis of the effect of the excitation amplitude F , the system backpressure P_b , mass block quality m and so on on the power generation voltage of the power trapping device.

For the power of different vibration amplitude frequency response under the curve as shown in figure 4, the curve in the figure shows that the transducer is the low frequency power device, when the external excitation frequency is less than 20 Hz, power generation capacity of harvester is affected by the amplitude of the excitation is more obvious, by increasing the amplitude of the external excitation mode, can be improved harvesting

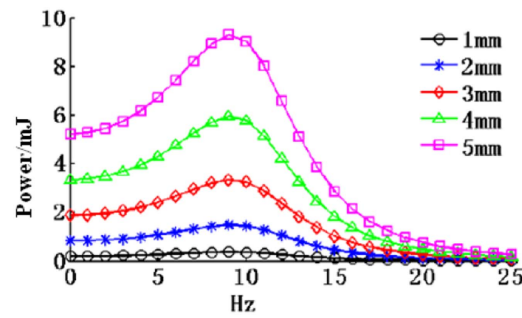


Figure 4. Frequency response curve of electric energy under different exciting amplitude.

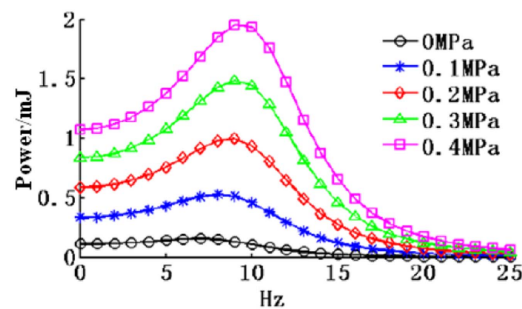


Figure 5. Frequency response curve of electric energy under different system back pressure.

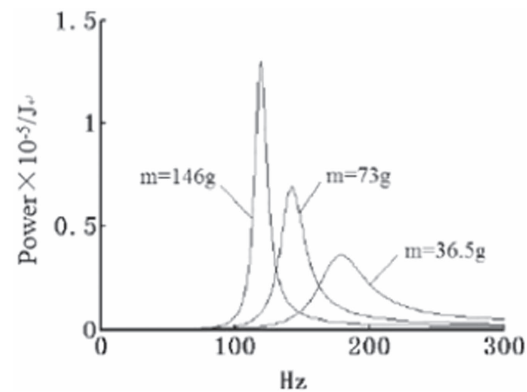


Figure 6. Relationship between power generation and excitation frequency under different mass quality.

capacity is put. For the peak frequency of the frequency response curve, the amplitude of the external excitation has no effect on the peak frequency. In order to study whether the external excitation amplitude affects the peak frequency, the feasibility will be discussed in the follow-up study.

For the system backpressure P_h is 0 MPa, 0.1 MPa, 0.2 MPa, 0.3 MPa, 0.4 MPa, change the excitation frequency ω value between 0–25 Hz, and get the frequency response curve of electric energy, as shown in figure 5.

By comparing the frequency response curves of the electric energy under different system back pressure, it can be seen that when the excitation frequency is below 20 Hz, the effect of the energy harvester in low frequency is more obvious. With the increase of the system backpressure and the power generation under the excitation frequency, the system back pressure has improved the power capacity, in which the peak value of the frequency response curve increases greatly, and the frequency is less affected by the system back pressure. After comparing and analyzing the curves, the increase of the preset pressure in the accumulator can reduce the compressibility of the fluid, and then reduce the energy loss and improve the power energy of the energy harvester.

Figure 6 shows the relationship between the power generation and the excitation frequency when the number of piezoelectric vibrators in the masses of different mass ($M = 36.5 \text{ g}, 73 \text{ g}, 146 \text{ g}$) is $n = 1$. The icon can be seen there

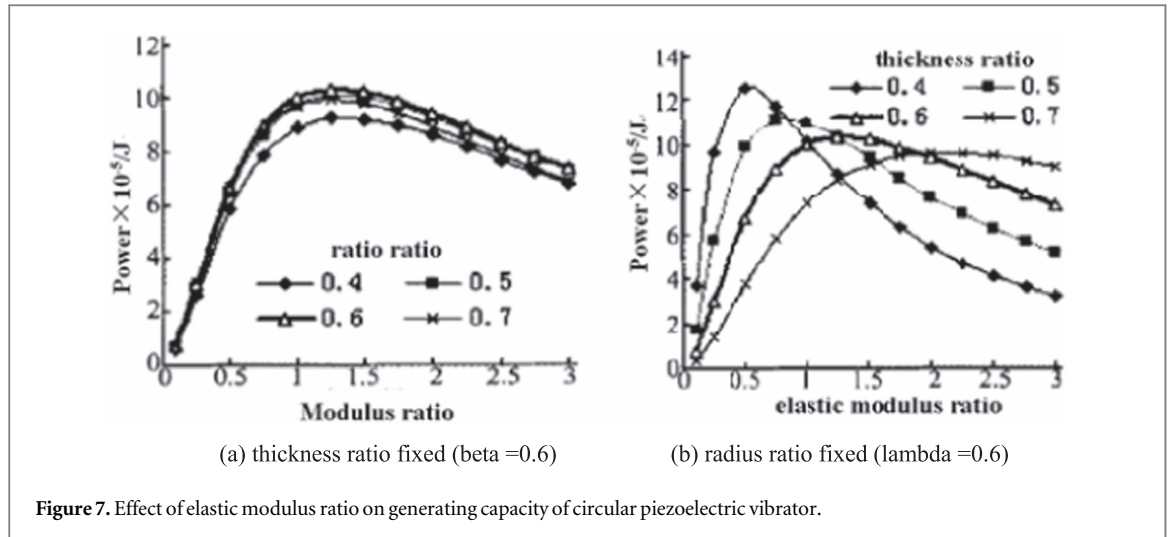


Figure 7. Effect of elastic modulus ratio on generating capacity of circular piezoelectric vibrator.

the best excitation frequency makes the generation ability of piezoelectric generator was the strongest, the best excitation frequency is the natural frequency of piezoelectric generator; with the increase of mass, natural frequency of piezoelectric generator is reduced, and the maximum power output increases with increasing mass.

The results of numerical simulation shows that basic vibration type multi vibrator series of natural frequency of piezoelectric generator is much lower than that of single crystal piezoelectric vibrator, strong adaptability to the natural environment of frequency, power performance.

According to the previous theoretical analysis, the displacement curve and the power generation capacity of the circular piezoelectric vibrator under concentrated load are also affected by piezoelectric ceramics and metal substrate materials. Figure 7 shows the influence of elastic modulus ratio of circular piezoelectric vibrator power generation capacity, shows that the variation of the curve in the figure, the piezoelectric vibrator of each structure size determine there is a optimal elastic modulus to the ratio of the maximum power output. To determine the optimum thickness ratio, elastic modulus ratio is less affected by the radius ratio, even no effect in figure 7(a); the radius ratio is determined, the optimal elastic modulus ratio with the thickness ratio decreases, but the corresponding power can improve the relative in figure 7(b). Figure 7(b) shown phenomenon lies in the generation of the piezoelectric vibrator is composed of elastic modulus ratio, radius ratio and thickness ratio determined: elastic modulus ratio, thickness ratio is not the same at the same time, the piezoelectric vibrator center composite layer stiffness, so that the stress and power generation; as for the piezoelectric vibrator thickness is relatively small due to the larger amount of power in its best elastic modulus ratio, mainly due to its freedom is one of the larger capacitance $C_f = \lambda^2 a^2 \pi / (\beta_{33}^S \beta h)$ (calculation method of power generation—see Formula (14)). Therefore, reducing the elastic modulus of the substrate helps to improve the generation capacity of the circular piezoelectric vibrator under concentrated load.

4. Simulation and analysis of electromechanical equivalent model

From the front we can see that the mechanical system model can be equivalent to the circuit model, so the mechanical structure model figure 1 of the liquid filled piezoelectric actuator can be equivalently analyzed by the circuit model.

The system is simplified into a dynamic model with an equivalent mass, an equivalent stiffness, and an equivalent damping. The calculation model and the mechanical circuit diagram of the whole system are shown in figure 8. If the mechanical impedance is taken as the displacement impedance, the displacement impedance of each element in the figure is:

$$\begin{aligned} Z_1 &= -\omega^2 m_1, \quad Z_2 = k_1, \quad Z_3 = k_2, \quad Z_4 = k_3, \quad Z_5 = i \cdot \omega \cdot c_1, \quad Z_6 = -\omega^2 m_f, \quad Z_7 = k_4, \\ Z_8 &= i \cdot \omega \cdot c_2, \quad Z_9 = k_5, \quad Z_{10} = i \cdot \omega \cdot c_3 \end{aligned} \quad (16)$$

Z_6 and Z_7 is reduced to Z_6^1 ,

$$Z_6^1 = Z_6 + Z_7, \quad (17)$$

Z_6, Z_7 is reduced to $Z_7^1, Z_7^1 = Z_8 + Z_9 + Z_{10}$

Z_6^1 and Z_7^1 is reduced to Z_6^2 ,

$$Z_6^2 = \frac{Z_6^1 \cdot Z_7^1}{Z_6^1 + Z_7^1}, \quad (18)$$

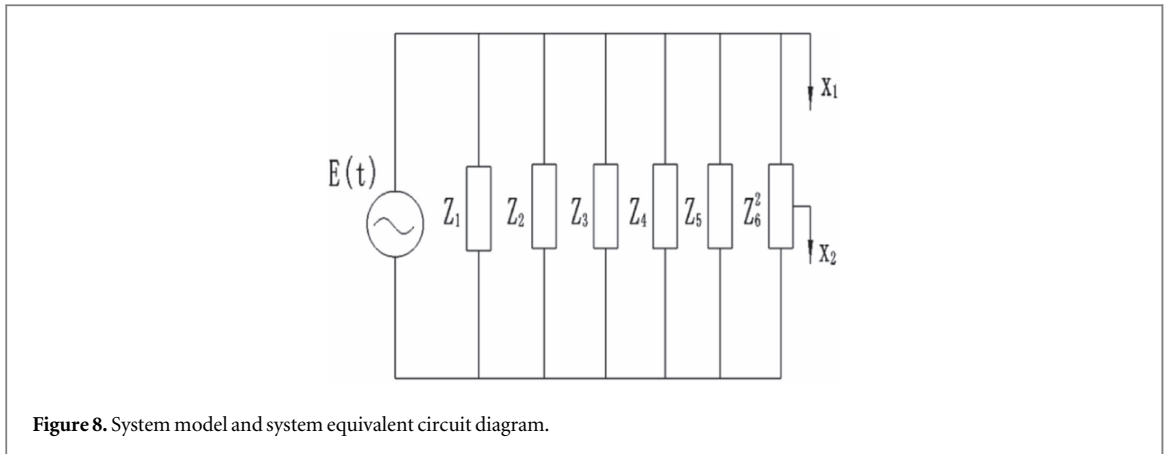


Figure 8. System model and system equivalent circuit diagram.

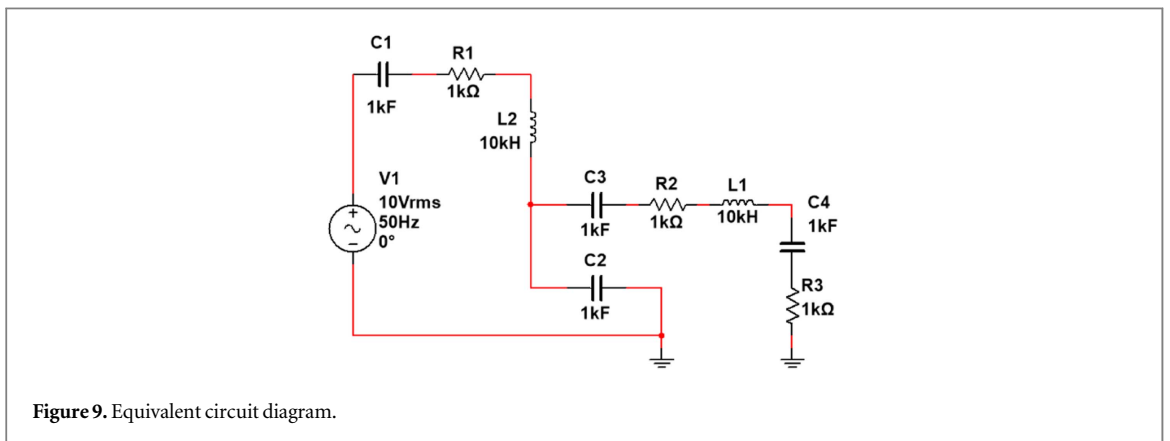


Figure 9. Equivalent circuit diagram.

$Z_1, Z_2, Z_3, Z_4, Z_5, Z_6^2$ is reduced:

$$Z_1^1, Z_1^1 = Z_1 + Z_2 + Z_3 + Z_4 + Z_5 + Z_6^2 \tag{19}$$

the displacement X_1 of node 1 in figure 8 is

$$\begin{aligned} x_1 &= \frac{E}{Z_1^1} = Z_1^1 = Z_1 + Z_2 + Z_3 + Z_4 + Z_5 + Z_6^2 \\ &= \frac{(Z_6 + Z_7 + Z_8 + Z_9 + Z_{10}) \cdot E}{[(Z_1 + Z_2 + Z_3 + Z_4 + Z_5) \cdot (Z_6 + Z_7 + Z_8 + Z_9 + Z_{10}) + (Z_6 + Z_7) \cdot (Z_8 + Z_9 + Z_{10})]} \end{aligned} \tag{20}$$

F_{Z1} of node 1 F_{Z1} and $F_{Z1} = x_1 \cdot Z_1$:

$$F_{Z1} = \frac{(Z_6 + Z_7 + Z_8 + Z_9 + Z_{10}) \cdot E \cdot Z_1}{[(Z_1 + Z_2 + Z_3 + Z_4 + Z_5) \cdot (Z_6 + Z_7 + Z_8 + Z_9 + Z_{10}) + (Z_6 + Z_7) \cdot (Z_8 + Z_9 + Z_{10})]} \tag{21}$$

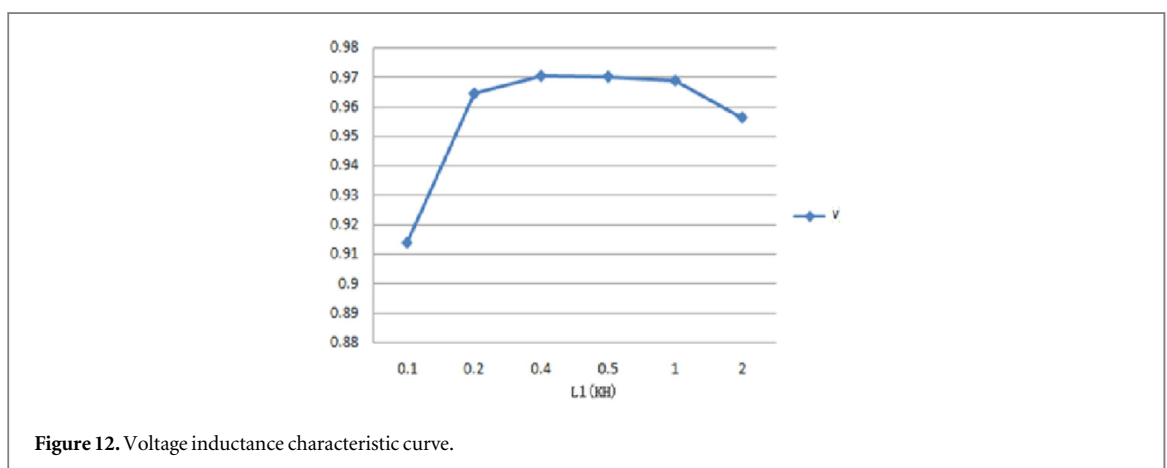
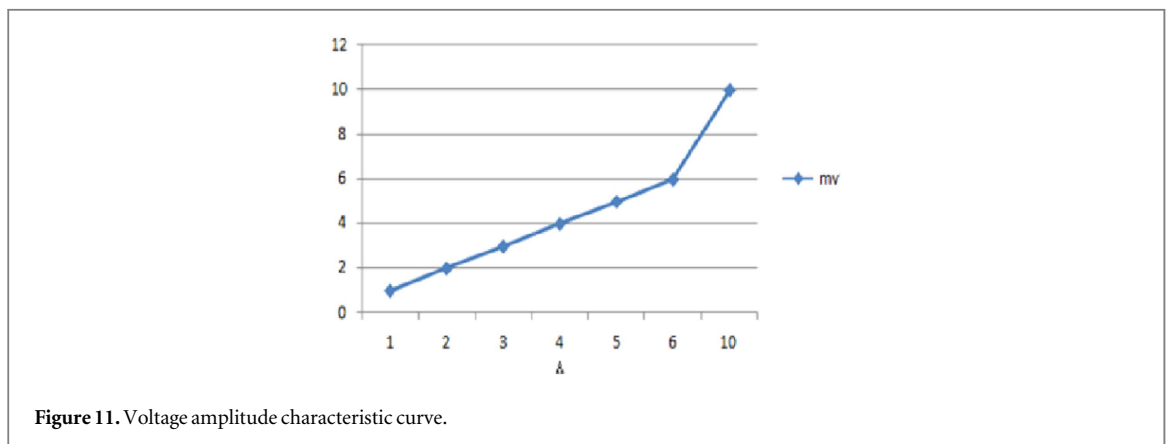
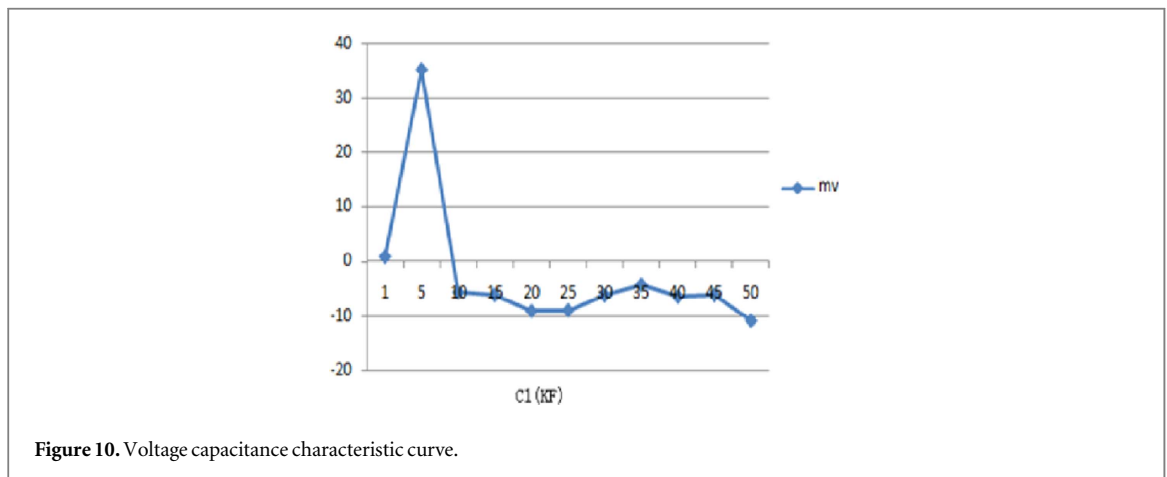
Thus, the expression of the passing rate V_a is given:

$$\begin{aligned} V_a &= \left| \frac{F_{Z1}}{E} \right| \\ &= \left| \frac{(Z_6 + Z_7 + Z_8 + Z_9 + Z_{10}) \cdot Z_1}{[(Z_1 + Z_2 + Z_3 + Z_4 + Z_5) \cdot (Z_6 + Z_7 + Z_8 + Z_9 + Z_{10}) + (Z_6 + Z_7) \cdot (Z_8 + Z_9 + Z_{10})]} \right| \end{aligned} \tag{22}$$

Substitute the values in formula (22):

$$\begin{aligned} V_a &= \left| \frac{F_{Z1}}{E} \right| \\ &= \left| \frac{(Z_6 + Z_7 + Z_8 + Z_9 + Z_{10}) \cdot Z_1}{[(Z_1 + Z_2 + Z_3 + Z_4 + Z_5) \cdot (Z_6 + Z_7 + Z_8 + Z_9 + Z_{10}) + (Z_6 + Z_7) \cdot (Z_8 + Z_9 + Z_{10})]} \right| \end{aligned}$$

The specific equivalent circuit diagram is shown in figure 9.



Through figures 10–12 analysis, figure 10 for different capacitor c_1 voltage curve, the capacitance between 1–50 KF, with the increase of capacitance voltage increased first and then decreased, the best capacitance of the inductance (L_2) power voltage reaches the maximum capacitance is 5 KF, the maximum power voltage is 35.178 mv; figure 11 shows the curve in the 1–10 V. Between the voltage increases with the increase of the amplitude of voltage curve; figure 12, inductance between 0–2 KH, with the increase of the inductor voltage increases first and then decreases, there is the best to reach the maximum inductance voltage, when the inductance is 0.4 kH, voltage is 0.970 55 mv, which is consistent with the analysis in the second chapter, the finite element simulation. Show that the circuit equivalent circuit designed in this paper can reflect the mechanical system model diagram.

5. Conclusion

This paper designs a kind of Piezoelectric liquid resistance capture energy device, by using the superposition theory of the sheet deformation, the calculation model of the displacement curve of the circular piezoelectric vibrator and the power generation capacity under the concentrated load is established. The results show that the radius ratio, thickness ratio and Young's modulus of the circular piezoelectric vibrator have greater influence on the power generation capacity. When the material of piezoelectric oscillator is determined, the best radius ratio and thickness ratio make the power generation capacity the largest. Excessive or small radius ratio and thickness ratio will reduce the generating capacity and even generate zero power. In addition, the electromechanical equivalent model is established. Equivalent analysis is made by changing the circuit impedance. The results are consistent with the theoretical simulation results, indicating that the established circuit model can truly reflect the characteristics of the theoretical model.

ORCID iDs

Li Zheng  <https://orcid.org/0000-0003-2443-3268>

References

- [1] Gilbert J M and Balouchi F 2008 Comparison of energy harvesting systems for wireless sensor networks *International Journal of Automation and Computing* **05** 334–47
- [2] Lei A, Xu R, Thyssen A, Stoot A C, Christiansen T L, Hansen K, Lou-Moller R, Thomsen E V and Birkelund K 2011 MEMS-based thick film PZT vibrational energy harvester [C] *MEMS 2011 (Cancun, MEXICO)* pp 125–8
- [3] Lee B S, Lin S C, Wu W J, Wang X Y, Chang P Z and Lee C K 2009 Piezoelectric MEMS generators fabricated with an aerosol deposition PZT thin film [J] *J. Micromech. Microeng.* **19** 065014
- [4] Aktakka E E, Peterson R L and Najafi K 2011 Thinned-PZT on SOI process and design optimization for piezoelectric inertial energy harvesting [C] *Transducer's 11 (Beijing, China)* pp 1649–52
- [5] Roundy S 2003 Energy scavenging for wireless sensor nodes with a focus on vibration to electricity conversion *PhD dissertation* U.S.A: University of California, Berkeley
- [6] Ottman G K, Hofmann H F, Bhatt A C and Lesieutre G A 2002 Adaptive piezoelectric energy harvesting circuit for wireless remote power supply [J] *IEEE Trans. Power Electron.* **17** 66–76
- [7] Anderson J, Semicigil S and Turan Ö 2000 An improved standing-wave-type sloshing absorber [J] *J. Sound Vib.* **235** 702–10
- [8] Marsh A et al 2010 A shallow-depth sloshing absorber for structural control [J] *Journal of Fluids and Structures* **26** 780792
- [9] Bai-Chang W U et al 2006 A novel piezoelectric hybrid ceramic solid-fluid actuator [J] *Piezoelectrics & Acousto-optics* **28** 677–9
- [10] Ehrenberg O and Kosa G 2012 Analysis of a novel piezoelectric micro-pump for drug delivery in a medical integrated micro system [C] *The Fourth IEEE RAS/EMBS Int. Conf. on Biomedical Robotics and Biomechanics (Roma, Italy, June 24-27)*
- [11] Fang X-Q, Zhu C-S and Liu J-X 2018 Surface energy effect on free vibration of nano-sized piezoelectric double-shell structures *Physica B: Physics of Condensed Matter* **529** 41–56
- [12] Zhu C-S, Fang X-Q, Liu J-X and Li H-Y 2017 Surface energy effect on nonlinear free vibration behavior of orthotropic piezoelectric cylindrical nano-shells *Eur. J. Mech. A* **66** 423–32
- [13] Zhu C-S, Fang X-Q and Liu J-X 2017 Surface energy effect on buckling behavior of the functionally graded nano-shell covered with piezoelectric nano-layers under torque *Int. J. Mech. Sci.* **133** 662–73
- [14] Deterre M, Lefeuvre E and Dufour-Gergam E 2012 An active piezoelectric energy extraction method for pressure energy harvesting [J] *Smart Materials & Structures* **21** 085004 -1-9
- [15] Delong J, Guangming C, Xiaofeng S and Zhigang Y 2010 Performance analysis and experimental study on delivery fluid of double-chamber piezoelectric pump in parallel *Journal of Xi'an Jiao Tong University* **44** 82–5
- [16] Zunqiang F et al 2010 The precision step driven motor driven by piezoelectric stack pump *China Journal of Electrical Engineering* **30** 106–11
- [17] Jung-Ho P, Kazuhiro Y and Shinichi Y 1999 Resonantly-driven-piezoelectric-micropump: Fabrication of a micro-pump having high power density [J] *Mechatronics* 687–702
- [18] Park J-H, Yoshida K, Nakasu Y and Yokota S 2002 A resonantly-driven piezoelectric micro-pump for micro-factory [J] *Proc. Of ICMT Kitakyushu*: pp 417–22
- [19] Rujun S et al 2016 A study of vortex-induced energy harvesting from water using Pzt piezoelectric cantilever with cylindrical extension [J] *Ceram. Int.* **41** 5768–73
- [20] Xiaobiao S et al 2015 Novel energy harvesting: a macro fiber composite piezoelectric energy harvester in the water vortex [J] *Ceram. Int.* **41** S763–7
- [21] Roundy S, Wright P K and Rabaey J 2003 A study of low level vibrations as a power source for wireless sensor nodes [J] *Comput. Commun.* **26** 1131–44
- [22] Mitsos A and Barton P I 2009 *Microfabricated Power Generation Devices: Design and Technology [M]* (Weinheim: Wiley-VCH)
- [23] Renaud M et al 2009 Harvesting energy from the motion of human limbs: the design and analysis of an impact-based piezoelectric generator [J] *Smart Mater. Struct.* **18** 035001
- [24] Pratiher B 2012 Vibration control of a transversely ex-cited cantilever beam with tip mass [J] *Arch. Appl. Mech.* **82** 3142
- [25] Jianwei W, Hui X and Cong J 2008 Numerical analysis of self-adaptive vibration suppression for flexible plate with imbedded fluid subsystem *Journal of Xi'an Jiao Tong University* **42** 613–6
- [26] Cheng J L and Hui X 2006 A research on nonlinear dynamic characteristic of vibro-impact system under harmonic excitation [J] *Journal of Materials and Structures* **1** 247–66

- [27] Jianwei W, Hui X and Ning M 2011 Investigation on self-adaptive vibration suppression for cantilever euler beam with interior inlaid fluid under principal resonance excitation *J. Vibration Shock* **30** 41–4
- [28] Junwu K *et al* 2011 Multi vibrator piezoelectric generator output characteristics of [J] *Optics and Precision Engineering* **19** 2108–16
- [29] Zheng L *et al* 2012 The fluid solid coupling effect of piezoelectric hydraulic vibration energy harvester based on [J] *Optics and Precision Engineering* **20** 1002–8
- [30] Delong J *et al* 2011 The research on piezoelectric cantilever oscillator generator performance *Mechanical Design and Manufacture* **1** 121–3